

Supplementary Information for: A comparative study on the morphological features of highly ordered MgO:AgO nanocube arrays prepared via hydrothermal method

K. Kaviyarasu^{1,2*}, E. Manikandan^{1,2,3}, J. Kennedy^{1,2,4}, M. Maaza^{1,2}

¹UNESCO-UNISA Africa Chair in Nanosciences/Nanotechnology Laboratories, College of Graduate Studies, University of South Africa (*UNISA*), Muckleneuk Ridge, P O Box 392, Pretoria, South Africa.

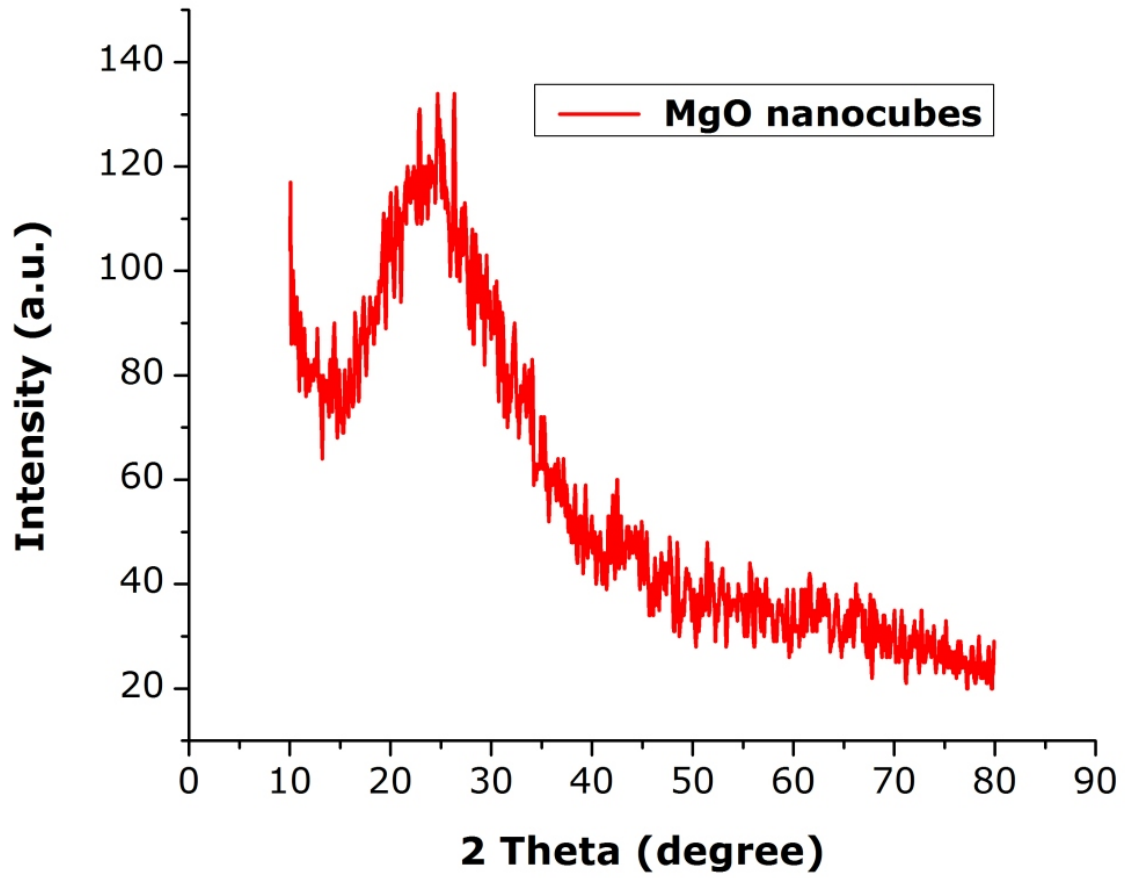
²Nanosciences African network (*NANOAFNET*), Materials Research Department (MSD), iThemba LABS-National Research Foundation (*NRF*), 1 Old Faure Road, 7129, P O Box 722, Somerset West, Western Cape Province, South Africa.

³Central Research Laboratory, Sree Balaji Medical College & Hospital, Bharath University, Chrompet, Chennai, Tamil Nadu, India, Pin -600044.

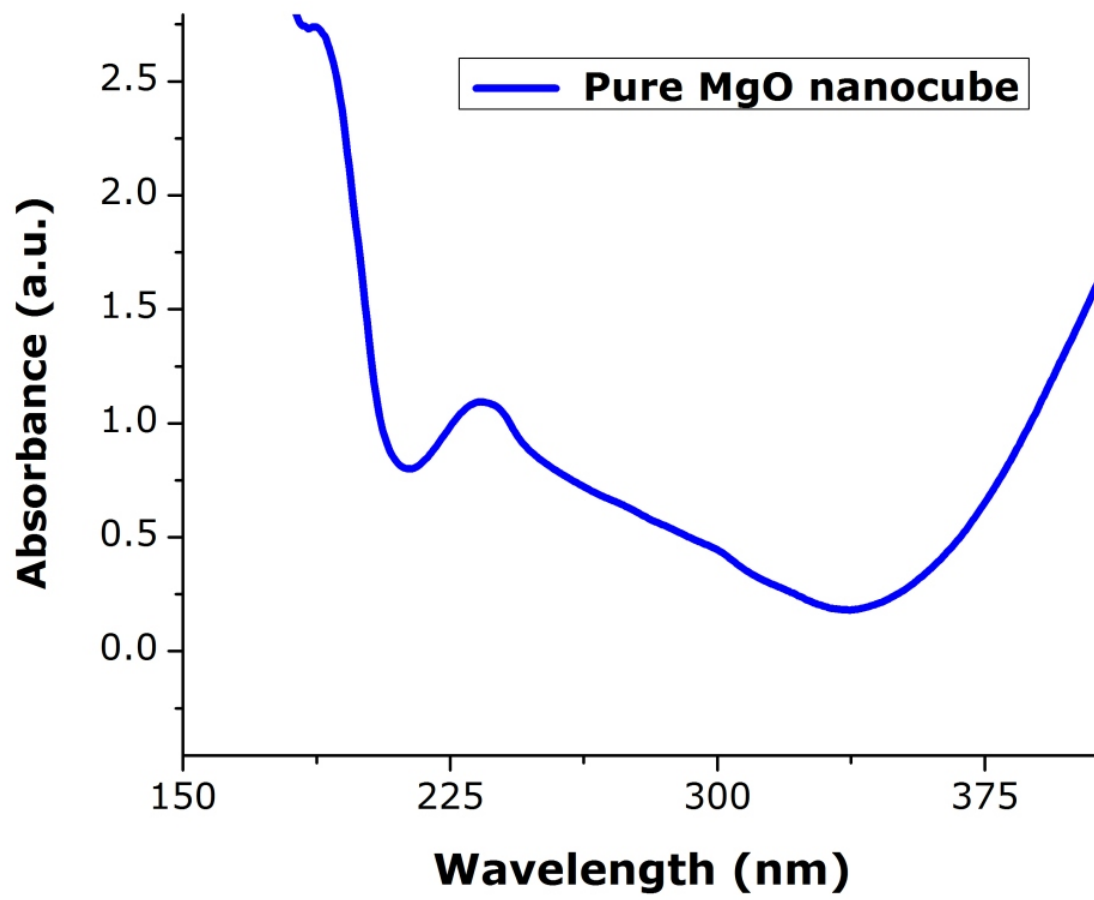
⁴National Isotope Centre, GNS Science, PO Box 31312, Lower Hutt 5010, New Zealand

¹ Corresponding author: Kaviyarasuloyolacollege@gmail.com; (K. Kaviyarasu), likmaaz@gmail.com (M. Maaza), Tel:- +27630441709.

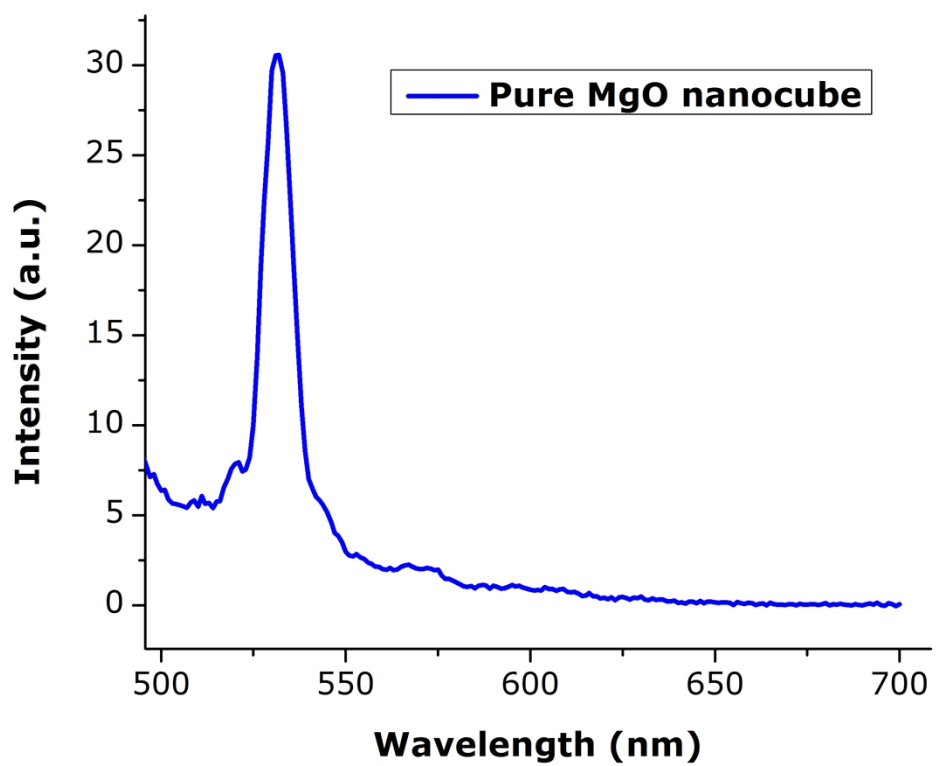
SUPPLEMENTARY FIGURES



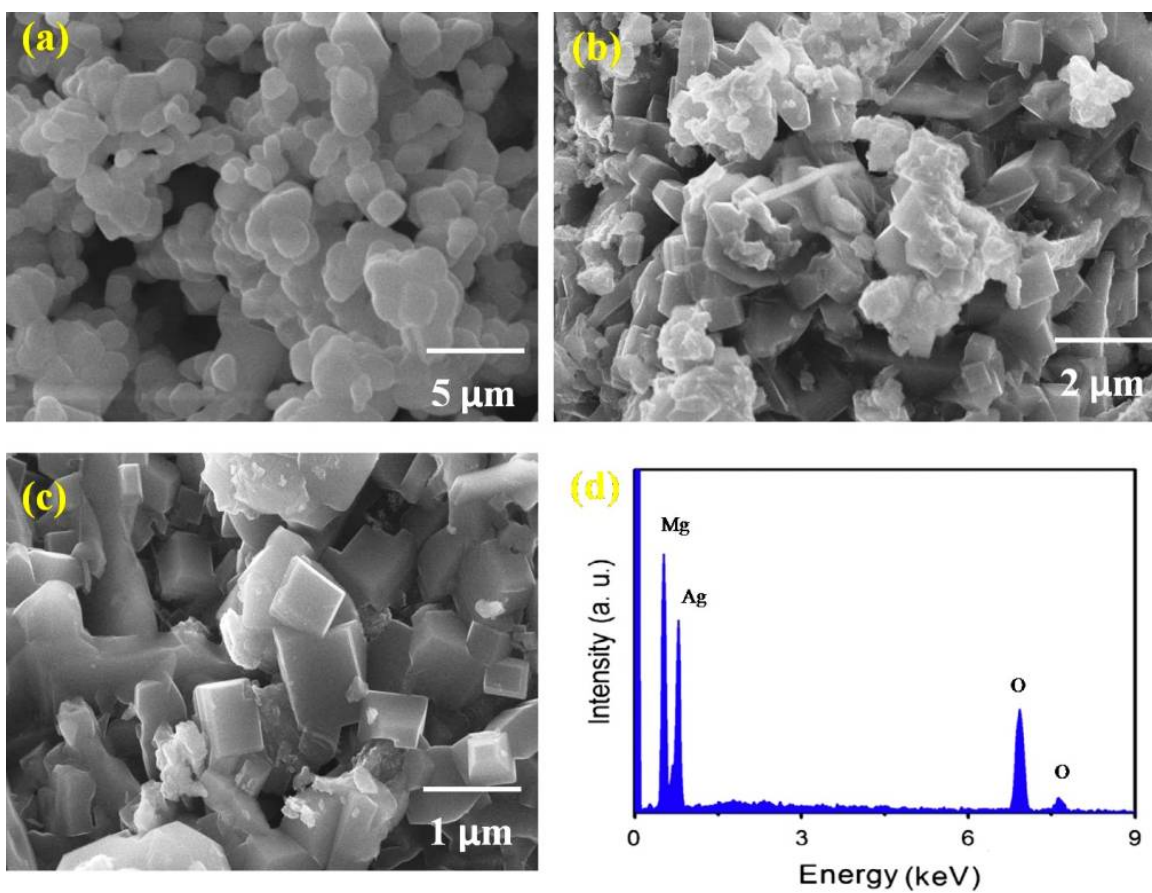
Supplementary Figure S1:- XRD pattern of pure MgO nanocube arrays prepared via hydrothermal method.



Supplementary Figure S2:- Optical absorption images of pure MgO nanocube prepared via hydrothermal method.



Supplementary Figure S3:- Photoluminescence spectrum when excited at 495 nm of pure MgO nanocube prepared via hydrothermal method.



Supplementary Figure S4:- Scanning electron microscopy (SEM) images and Energy dispersive spectrum (EDS) pattern of pure MgO nanocube prepared via hydrothermal method.

Supplementary Discussions

Figure S1:

The spectrum reflects the good crystallinity for MgO nanosamples. The broadness of the XRD peaks indicates the nanocrystalline nature of MgO nanoparticles. The Bragg's reflections are indexed in MgO like cubic structure and the estimated cell constant a is ($a = 4.21 \text{ \AA}$) of MgO particles confirms that the sample is formed in a single phase. The cell constant is slightly less than that of MgO nanosample which may be due to the introduction of MgO ($a = 4.46 \text{ \AA}$). Considerably broadened lines in the XRD patterns are indicative of the presence of nano-size particles. We have used the (200) reflection, like in the XRD patterns, for obtaining the average particle size with the help of Debye - Scherrer's equation $t = 0.9 \lambda / B \cos \theta$, $B = (BM_2 - BS_2)^{1/2}$ where 't' is the thickness (diameter) of the particle, λ is the X-ray wavelength (1.5418 \AA), BM and BS are respectively the measured peak broadening and the instrumental broadening in radian and ' θ ' is the Bragg angle of the reflection. The calculated average particle sizes ranged between 20 and 23 nm. The XRD pattern of regenerated MgO powder ascertains an MgO sample is a nanocrystalline material.

Figure S2:

The spectra were recorded for IR, visible and UV region. From the absorption peak, the optical band gaps were calculated and the natures of transitions were also identified. The spectra are shown in Fig. S2. From the spectra, it is evident that the absorbance is not registered due to its excellent optical behavior from 300 nm to 900 nm. Negligible absorption in the region between 495 to 700 nm is an added advantage, as it is the key requirement for nanomaterials having NLO properties. Energy band gap (E_g) of materials is related to absorption coefficient (α) or $(\alpha h\nu) = A (h\nu - E_g)^n$ where 'A' is a constant, ' $h\nu$ ' is the photon energy, ' E_g ' the band gap and 'n' is an index which assumes the values of 1/2, 3/2, 2 and 3 depending on the nature of the electronic transition responsible for the absorption $n = 1/2$ is taken for an allowed direct transition. The extrapolation of the straight line gives the value of the energy band gap. The energy band gaps for MgO nanoparticles were found to be 1.7 and 2.5 eV. From the data it clear that the shift in the band gap of nanoparticle is due to the quantum confinement.

Figure S3:

The photoluminescence studies are carried out to detect the lower concentration of defects. The photoluminescence studies are preferred rather than the optical absorption. This is a mechanism where the impurity on absorption of light, gives rise to the bound excited state from which it returns to its ground state abiding in accordance with the color centre creation mechanism. The room temperature photoluminescence spectra of MgO nanosamples are shown in Fig. 3. When the excitation wavelength is 270 nm, for peaks are observed at 400, 450 and 475 nm respectively. The peak at 450 nm can be attributed to the relaxation of polarization defects formed by the strained sites attached to oxygen vacancies. Oxygen vacancy which might be the common defect in the nanosamples induces distortion of the lattice in its direct surrounding. In case of our samples, the red shift in the MgO is slightly enhanced. Therefore, red shift of the photoluminescence peaks is a result of band gap reduction. Such a characteristic is vital for enhancement of secondary electron emission efficiency, reduction of flickering, etc. Therefore this optical property is promising for its application in plasma display panels (PDP) or other optical fields.

Figure S4:

The scanning electron microscopy (SEM) measurement was carried out using JSM 840-A SEM instrument in order to analyze the structure and morphology of synthesized samples. The instrument was accelerated with a voltage of 20 kV and the samples were scanned at a working distance of 15 mm. The samples were dispersed in isopropyl alcohol and scanned with a magnification of 10,000x. The SEM images for the MgO samples are shown in Fig. S4. From the SEM images the particle sizes of the pure MgO nanocrystals were found to be in the range 10 μm to 1 μm , which is in accordance with the reported value. It is also clear that the synthesized MgO sample is very porous with large pores and open voids.

Supplementary References

- [1] K. Kaviyarasu, E. Manikandan, J. Kennedy, M. Jayachandran, Quantum confinement and photoluminescence of well-aligned CdO nanofibers by a solvothermal route, *Mat. Lett.* 120 (2014) 243-245.
- [2] J.A. Farmer, C.T. Campbell, L. Xu, G. Henkelman, Defect Sites and Their Distributions on MgO (100) by Li and Ca Adsorption Calorimetry, *J. Am. Chem. Soc.* 131 (2009) 3098-3103.
- [3] M.S. Melgunov, V.B. Fenelonov, A partial surface area measurement method for multicomponent catalysts and adsorbents, *React. Kin. Cat. Lett.* 64 (1998) 153-160.
- [4] Susumu Takahashi, Yusuke Imai, Akinori Kan, Yuji Hotta, Hirotaka Ogawa, Improvements in the temperature-dependent properties of dielectric composites by utilizing MgO whiskers as the dielectric filler in an iPP matrix, *J. Alloys & Comp.* 640 (2015) 428–432.
- [5] D.C. Pereraa, W.J. Hewagea, N.D. Silva, Theoretical study of catalytic decomposition of acetic acid on MgO nanosurface, *Comp. Theoretical Chem.* 1064 (2015) 1–6.
- [6] K. Kaviyarasu and Prem Anand Devarajan, Synthesis and characterization studies of cadmium doped MgO nanocrystals for optoelectronics application, *Pel. Res. Lib. Adv. App. Sci. Res.* 2 (2011) 131-138.
- [7] K. Kaviyarasu and Prem Anand Devarajan, A versatile route to synthesize MgO nanocrystals by combustion technique, *Sch. Res. Lib. Der. Pharma. Chemica.* 3 (2011) 248-254.